# CHAPTER-VII

## PHYSICOCHEMICAL INVESTIGATION TO PROBE THE RECOVERY AND CONTROLLING MANAGEMENT OF GOUT PAIN IN HUMAN BODY THROUGH ACCUMULATION OF VITAMIN $B_6$ MOLECULE

### 7.1. Introduction

Pyridoxal 5'-phosphate (PLP) is biochemically considered as the active form of vitamin B6. We know enzymes use an array of organic cofactors to catalyze demanding chemical reactions under physiological situations. Amongst these all cofactors, pyridoxal-phosphate (PLP), active form of Vitamin B6, and is one of the most adaptable. It is vital in metabolism of carbohydrates, amino acids, fatty acids, neurotransmitters (serotonin, nor epinephrine), sphingolipids, and aminolevulinic acid. It plays an important role in living organisms, and humans and animals must obtain it from food.

Gout is a pictorial presentation of uric acid disturbance described by type of arthritis, hyperuricemia, acute and chronic allow for an even enhanced understanding of the disease. It is a systemic disease which results from deposition of monosodium urate crystals in tissues. World-wide rate of gout have increased gradually owing to poor dietary habits such as fast foods, increased incidence of obesity, lack of exercises and metabolic syndrome.

Deficiency of enzymes involved in purine metabolism leads to overproduction of UA. Vitamins were found to increase renal excretion of uric acid so it can be used as a supplement during management of gout. Therefore Vitamins were interacted with the uric acid in this paper to show their stability and utility in the human body at diverse temperatures by various physicochemical contrivances [1-7].

### 7.2. Experimental Section

#### 7.2.1 Materials and Methods

The compound under investigation namely PLP and Uric acid (UA) are purchased from Sigma–Aldrich chemicals, USA which are of spectroscopic grade and hence used for recording the spectra as such without any further purification All the solutions were all set in doubly distilled water on a molality basis using Mettler Toledo AG-285 with having accuracy of ±0.1 mg and uncertainty 0.0001 g.

Prior to the start of experimental work solubility of UA and PLP have been specifically checked in distilled water and observed that the selected aqueous UA was freely soluble in all proportion of PLP. Every stock solution of UA were set by mass (weighed by Mettler Toledo AG-285 with uncertainty 0.0003 g), and then working solutions were obtained by mass dilution at 298.15 K. Aqueous UA binary solution used as binary solvent system. The uncertainty within molality of solutions evaluated to ±0.0001 mol $kg^{-3}$. Solution densities (ρ) were dignified by vibrating-u-tube Anton Paar digital density meter (DMA 4500M) by a precision of 0.00005 g $cm^{-3}$ maintained at ±0.01 K.

In support of viscosity (η) suspended Ubbelohde viscometer was used and temperature of the experimental bath was maintained constant up to ±0.002 K, by circulating coolant liquid three different temperatures, viz., T = (298.15, 303.15 and 308.15) K has been measured [8].

In Conductance measurements Systronics Conductivity-TDS Meter 308 was used. Earlier to the experiment, cell constant and specific conductance of the solvent ($H_2O$) were measured and cell constant was found to be 0.10 $cm^{-1}$.

Digital Refractometer Mettler Toledo was used to determine refractive index. The refractometer was fixed by distilled water and calibration was tested after each few measurements.

Infrared spectra record was taken in 8300 FT-IR spectrometer (Shimadzu, Japan) and the particulars about this instrument have been illustrated in the literature [9].

UV spectra of different solutions, PLP and UA were obtained by Agilent 8453 UV-Vis spectrophotometer with uncertainty ±2 nm. A conventional 1 cm path (1 cm ×1 cm × 4 cm) quartz cell has been used. Scanning of the samples was taken within range from 190 to 1200 nm.

NMR spectra were taken in $D_2O$ using Bruker AV-300 spectrometer operating for 1H at 300 MHz. Chemical shifts (δ) were report in parts per million (ppm) relative to TMS as internal standard ($D_2O$: δ 4.79 ppm).

### 7.3. Results and discussion

#### 7.3.1. Density Correlation.

The experimental densities of vitamin B6 in aqueous solutions of UA at T = (298.15, 303.15 and 308.15) K are listed in Table 1. Comparison between experimental densities and

viscosities of vitamin B6 in aqueous solutions of UA shows variation tendencies of experimental densities and viscosities with molality show good agreement with literature values. It could be seen from Table 1 that densities of all solutions increase with the molality but decrease with increasing temperature. For the same solute, the densities increase monotonously with the molality of UA. While for the same molality of UA, the densities of all solutions increase with the molar weight of PY (see Figure 1).

Figure 1 intensely presents the relationship of the densities of PY versus temperature and solute molar concentration. It is observed that from Figure 1, densities of solutions show good linear relationship to the molar concentration of PY [10-14].

## 7.3.2. Volumetric Properties.

The apparent molar volumes of vitamin B6 in UA solutions were computed by the following relation:

$$\phi_V = M/\rho \; - \left(\rho - \rho_o\right)/m\rho_o\rho \qquad (1)$$

Where M molar mass of the salt, m is the molarity of the solution, $\rho$ and $\rho_0$ are density of the PY-UA solution and aq. UA mixture respectively.

The calculated apparent molar volumes are also included in Table 1. Figure 2 shows the plot of apparent molar volumes of PY in mol fractions of UA aqueous solutions at 298.15 K, 303.15K, and 308.15K. It is found that the apparent molar volumes vary linearly with molar concentration of the solute molecule.

Apparently, from Table 7.1, t all positive values with increase in temperature, which gives an insight that there exists the solute−solvent interaction and higher temperature could facilitate this kind of interaction. When the molality of UA aqueous solutions climbs, corresponding values of will also escalate under the specified temperature. Additionally, it could also be found that of PY under the condition of infinite dilution, the interactions between solute and solute is negligible, therefore, the solute− solvent interactions would become dominated in the solutions. Thus it could provide much valuable information about solute− solvent interactions [15].

## 7.3.3 Viscosity Measurement.

The experimental viscosities of vitamin B6 (PY) in uric acid (UA) aqueous solutions at T = (298.15, 303.15 and 308.15) K are displayed in Table 2a and partly depicted in Figure

2a. It could be clearly found from Figure 7.2 that the viscosities are in linear relationship to the molar concentration of solute. In this work, Jones-Dole equations were utilized to correlate the viscosities of solution.

The viscosity records for the calculated systems are listed in (Table7.2).

$$(\eta/\eta_o - 1)/\sqrt{m} = (\eta_r - 1)/\sqrt{m} = A + B\sqrt{m} \quad (2)$$

Where $\eta$ , $\eta_o$ are, viscosity of ternary (PY + aq. UA) system and binary aqueous UA mixture relative viscosity $\eta_r=\eta/\eta_o$ and m is the molarity of ternary solutions. A, B are empirical constants known as viscosity A- and B-coefficients, which identifies to solute-solute, solute-solvent interactions respectively. The values of A and B-coefficients are reported in (Table 2b).

In this experiment we found A-coefficient increases marginally with the increase in mass of PY in the solvent mixture represents very weak solute-solute interactions.

Viscosity *B*-coefficient gives information concerning solvation of solvated solutes and their effects on arrangement of solvent in local vicinity of the solute molecules in solutions. It is found that values of the *B*-coefficient presented in (Table 7.2) are positive and much higher rather than *A*-coefficient, suggesting solute-solvent interactions are superseding over the solute-solute interactions. (Table 7.1 and 7.2) shows values of *B* coefficients of PY decreases with increasing temperature (Figure7.2) [16, 17].

**7.3.4. Conductivity measurements**

For conductivity measurements at temperature 298.15 K for determination of break point for each solvent composition was carried out by plotting conductivity against the total concentration of the solution. The conductivity of a solution depends on solvation of its ions in it which involves types of intermolecular interactions: hydrogen bonding, ion-dipole interactions, and van der Waals forces. Measured specific conductance of solutions of the solute PY in UA- water 298.15K has been subjected for solvent correction and used to calculate molar conductance, $\lambda_m$ using equation

$$\lambda_m = k/C \quad (3)$$

Where *C* is the molar concentration of PY solution and κ is the measured specific conductance. The molar conductance ( $\Lambda$ ) of PY in different concentration of UA solutions were calculated at the corresponding molar concentrations given in Table 7.3. From the

perusal of Figure3 it is evident that conductance is higher in case of PY when 10mM of it is mixed with 2*10^ (-5) m solution. The molar conductance of PY is decreased with increasing the conc. of UA. The fact is due to the interaction of these charged species with the molecules by hydrogen bonding, which probably construct association by electrostatic forces, these consequences in the shrinks in the electrostatic attraction in PY and the molar conductances for the solution decreases (Scheme7.2) [18, 19].

### 7.3.5. Refractive Index

$R_{M,}$ molar refraction can be evaluated from Lorentz-Lorenz relation,

$$R_M = \{(n_D^2 - 1) / (n_D^2 + 2)\}(M / \rho) \quad (4)$$

$R_M$ = molar refraction

$n_D$ = refractive index

$M$ molar mass

$\rho$ = density of solution

Moreover limiting molar refraction ($R^0_M$) estimated from the following equation,

$$R_M = R^0_M + R_S\sqrt{m} \quad (5)$$

The refractive index in addition convenient method for investigating interaction happening in the electrolytic solution. Stated more briefly, by Deetlefs et al. that refractive index describes its capability to refract light as it moves from one medium to another and thus, higher refractive index of a compound, maximum light is refracted. Higher refractive index, higher molecules are more tightly packed or in general when the compound is denser. The refractive index is directly proportional to molecular polarizability, scrutiny of Table 4, Figure 4 reveals the $n_D$ and $R_M$ values increases with an increasing concentration of mass fraction PY into the solution of the used solvents, suggesting that in the UA and water medium it is more tightly packed and more solvated. This is also in best agreement with the results obtained from apparent molar volume and viscosity *B*-coefficient discussed above [20].

### 7.3.6 FTIR spectral determination

In case of pure pyridoxine phosphate all the major band assignments are represented at 3416.52 $cm^{-1}$ for stretching in phenolic –OH, 3239.85 $cm^{-1}$ for stretching in alcoholic –OH, 1646.42 $cm^{-1}$ and 1556.20 $cm^{-1}$ C=C and C=N aromatic ring stretch, 1275.22 $cm^{-1}$ is the C=O stretching of aryl alkyl group ether, 1246.04 $cm^{-1}$ is the C-O stretch in the vinyl ether,

1042.10 $cm^{-1}$ is the C-O is the stretch of the primary alcoholic group are the following peaks overviewed in the study; which relates with the interactions.

FTIR spectra of UA Shows a broad band around 3432.24 $cm^{-1}$ corresponding to NH stretching, shows a red shift as a consequence of hydrogen bonding. A band at 1673.66 $cm^{-1}$ is also observed from the template UA represents C=O stretch.

When the PY-UA-$H_2O$ combined ternary system it is observed the position of the vibrations are shifted or changed more in comparable to that of pure PY like 3416.52 $cm^{-1}$ for stretching in phenolic –OH is changed to 3419.41 $cm^{-1}$ in PY-UA-$H_2O$ system, 1646.42 $cm^{-1}$ for C=C aromatic ring stretch of pure PY is shifted to 1676.62 $cm^{-1}$, 1556.20 $cm^{-1}$ for C=N aromatic ring stretch is changed to 1590.78 $cm^{-1}$ and 1278.73 $cm^{-1}$ is the change noted for the ether group (Figure 5), which again proves the fact the interactions with pyridoxine phosphate, is best suited with uric acid [21-22].

**7.3.7 UV spectroscopy**

Pyridoxal phosphate is an important co-enzyme, but its precise structure has been very uncertain. Judgment of absorption curve of authentic co-enzyme with those of substances of established structure should be crucial. From literature recorded an absorption peak at 292 mp at pH 2.1 for pyridoxine phosphate and gradually decreases in intensity with decreasing hydrogen ion concentration; at pH values of 4 to 5 two new maxima appear at 255 and 326 mp. Whereas at pH 6.75, 292-mp peak is no longer shown and the 326-mp peak becomes very strong. As pH was changed from 6.75 to 10.2 the “alkaline” bands were displaced to 246 and 311 mp. Harris and Folkers invoked the ionic forms with the zwitterions part. Accordingly, the spectra of pyridoxine phosphate over a wide range of pH values have been determined.

In the present assay we have interpreted the pure form of pyridoxine phosphate with UA. We found the difference between Figure 6a and 6b, which judged the fact that around pH values of 4 in the acidic medium the interaction of PY is possible with UA in the aqueous phase when the concentrations of PY and UA are taken in the range of 10MM and 100MM.

The investigation illustrates spectrophotometric analysis of solute-solvent interaction systems and, in addition, confirms the established structure of codecarboxylase (pyridoxal phosphate) [23].

### 7.3.8 1H-NMR

In case of 1H-NMR though we cannot compare the extent of H-bonding (Scheme 1) but we can conform the positioning of H-bonding, if we have tally both system's i.e., pure PY and mixture of PY-UA. We have recorded 1H NMR spectra in $D_2O$ for exchangeable protons of four pyridoxal phosphate. A number of well resolved peaks, in Figure 7.1, show that the singlets and quartet around 2.5 ppm due to the protons of C-$CH_3$, $CH_3$ has shifted in Figure 7.3. C-OH peak around 3.315 ppm has also shifted in the lower region in the mixture. C-COH, HCO singlets and doublet of the pure PY is shifted in Figure 7c from 5.070-5.077ppm. The peak at 5.293 ppm for C-$CH_2$ in Figure 7.1 is present, whereas these peak is absent in Figure 7.3 which indicate that the proton in these region might have participated in hydrogen bonding. O-$PO_3H_2$ in Figure 7a shows triplets around 6.659 ppm, which is again absent in Figure 7.3. CH doublets are clearly observed in Figure 7.3 around 8.118 ppm which indicates that it is not involved in the interaction. Moreover the peak at 3.258 ppm in UA (Figure 7.2) for C=O is merged in the mixture. The proposed interaction has now been investigated and proved with high resolution 1H nuclear magnetic resonance spectroscopy [24].

## 7.4 Conclusion

Our studies have demonstrated a novel interaction between PY and UA, which would trigger the vitamin. It is seen whether individuals suffering with Gout, which is a kind of arthritis could be treated with vitamin B6 which would act as a co-enzyme, along with vitamin C studied earlier in the literature to firmly attract the uric acid crystals, and remove it from the body. As it is proved in these portray that in the acidic medium there is effective binding between PY and UA. It would also be important biologically to conjugate in their blood and urine.

## Abbreviations

Vitamin B6: (PY)

Uric acid: (UA)

# Tables

**Table 7.1. Density (ρ), apparent molar volume ($\phi_v$) of an aqueous solutions of UA in pyridoxine at different temperatures T = (298.15, 303.15 and 308.15) K at $10^5$ N. $m^{-2}$.**

| SOLUTION | $10^{-3}$ ρ/kg. $m^{-3}$ | | | $\phi_v * 10^6$ $m^3 \cdot mol^{-1}$ | | |
|---|---|---|---|---|---|---|
| | 298.15K | 303.15K | 308K | 298.15K | 303.15K | 308K |
| PURE 1*10^(-5) | 0.9972 | 0.9958 | 0.9942 | 0.011282 | 0.011297 | 0.011316 |
| 1ST | 0.9973 | 0.9959 | 0.9943 | 0.022563 | 0.022595 | 0.022631 |
| $2^{ND}$ | 0.9975 | 0.9961 | 0.9945 | 0.033849 | 0.033897 | 0.033951 |
| $3^{RD}$ | 0.9976 | 0.9962 | 0.9946 | 0.045126 | 0.045189 | 0.045262 |
| $4^{TH}$ | 0.9978 | 0.9964 | 0.9948 | 0.0677 | 0.067787 | 0.067896 |
| $5^{TH}$ | 0.9978 | 0.9965 | 0.9949 | 0.082475 | 0.082581 | 0.082732 |
| $6^{TH}$ | 0.9979 | 0.9966 | 0.9949 | 0.0845678 | 0.0871234 | 0.0888897 |
| | | | | | | |
| PURE 2*10^(-5) | 0.9972 | 0.9958 | 0.9942 | 0.013558 | 0.013539 | 0.013571 |
| 1ST | 0.9973 | 0.9959 | 0.9944 | 0.027115 | 0.027077 | 0.027158 |
| $2^{ND}$ | 0.9975 | 0.9961 | 0.9945 | 0.040685 | 0.040628 | 0.04075 |
| $3^{RD}$ | 0.9976 | 0.9962 | 0.9946 | 0.054234 | 0.054165 | 0.054321 |
| $4^{TH}$ | 0.9977 | 0.9964 | 0.9948 | 0.070075 | 0.069977 | 0.070188 |
| $5^{TH}$ | 0.9979 | 0.9965 | 0.9949 | 0.081327 | 0.081223 | 0.081467 |
| $6^{TH}$ | 0.998 | 0.9967 | 0.995 | 0.0834557 | 0.0823487 | 0.0832176 |
| | | | | | | |
| PURE 3*10^(-5) | 0.9972 | 0.9958 | 0.9942 | 0.011282 | 0.011287 | 0.011316 |
| 1ST | 0.9973 | 0.996 | 0.9943 | 0.022563 | 0.022595 | 0.022631 |
| $2^{ND}$ | 0.9975 | 0.9961 | 0.9945 | 0.033849 | 0.033897 | 0.033951 |
| $3^{RD}$ | 0.9976 | 0.9962 | 0.9946 | 0.045126 | 0.045189 | 0.045262 |
| $4^{TH}$ | 0.9978 | 0.9964 | 0.9948 | 0.067692 | 0.067779 | 0.067896 |
| $5^{TH}$ | 0.9979 | 0.9966 | 0.9949 | 0.072465 | 0.072567 | 0.076949 |
| $6^{TH}$ | 0.9981 | 0.9967 | 0.9950 | 0.0814532 | 0.867882 | 0.081125 |

**Table 7.2 Viscosities (η) of Vitamin B6 in aqueous Solution of Uric acid at T = (298.15, 303.15, 308.15) K and Pressure p = 101.3 kPa**

| For 1*10^(-5)m solutions | | | | | | | |
|---|---|---|---|---|---|---|---|
| Solution | C (mol. L-1) | η(m Pa.s) at 298.15K | $\eta_r$ at 298.15K | η(m Pa.s) at 303.15K | $\eta_r$ at 303.15K | η(m Pa.s) at 308.15K | $\eta_r$ at 308.15K |
| Pure | 0.00425 | 4.46 | | 4.44 | | 4.42 | |
| 1st | 0.01126 | 4.47 | 1.00224 | 4.45 | 1.00225 | 4.43 | 1.00226 |
| 2nd | 0.02252 | 4.48 | 1.00223 | 4.46 | 1.00224 | 4.44 | 1.00225 |
| 3rd | 0.03378 | 4.49 | 1.00223 | 4.47 | 1.00224 | 4.45 | 1.00225 |
| 4th | 0.04504 | 4.5 | 1.00222 | 4.48 | 1.00223 | 4.46 | 1.00224 |
| 5th | 0.06756 | 4.51 | 1.00222 | 4.49 | 1.00223 | 4.47 | 1.00224 |
| 6th | 0.08231 | 4.52 | 1.00221 | 4.5 | 1.00222 | 4.48 | 1.00223 |
| For 2*10^(-5)m solutions | | | | | | | |
| Pure | 0.0054 | 4.48 | | 4.46 | | 4.44 | |
| 1st | 0.01351 | 4.49 | 1.00223 | 4.47 | 1.00224 | 4.45 | 1.00225 |
| 2nd | 0.02702 | 4.5 | 1.00222 | 4.48 | 1.00223 | 4.46 | 1.00224 |

| | | | | | | | |
|---|---|---|---|---|---|---|---|
| 3rd | 0.04054 | 4.51 | 1.00222 | 4.49 | 1.00223 | 4.47 | 1.00224 |
| 4th | 0.05405 | 4.52 | 1.00221 | 4.5 | 1.00222 | 4.48 | 1.00223 |
| 5th | 0.06984 | 4.53 | 1.00221 | 4.51 | 1.00222 | 4.49 | 1.00223 |
| 6th | 0.08107 | 4.54 | 1.00220 | 4.52 | 1.00221 | 4.5 | 1.00222 |
| For 3*10^(-5)m solutions | | | | | | | |
| Pure | 0.045 | 4.53 | | 4.48 | | 4.46 | |
| 1st | 0.01126 | 4.54 | 1.00220 | 4.49 | 1.00223 | 4.47 | 1.00224 |
| 2nd | 0.02252 | 4.55 | 1.00220 | 4.5 | 1.00222 | 4.48 | 1.00223 |
| 3rd | 0.03378 | 4.56 | 1.00219 | 4.51 | 1.00222 | 4.49 | 1.00223 |
| 4th | 0.04504 | 4.57 | 1.00219 | 4.52 | 1.00221 | 4.5 | 1.00226 |
| 5th | 0.06756 | 4.58 | 1.00218 | 4.53 | 1.00221 | 4.51 | 1.00222 |
| 6th | 0.07234 | 4.59 | 1.00218 | 4.54 | 1.00220 | 4.52 | 1.00221 |

m stands for the molality of vitamin B6 in (UA + water) mixture solvents. Standard uncertainty: in molality u(m) = ± 1·10−4 mol·kg−1 ; u(T) = ± 0.02 K; in viscosities u(η) = ± 1%, u(T) = ± 0.02 K.

**Table 7.3** $(\eta_r - 1)/\sqrt{m}$**, Viscosity *A*- and *B*-coefficients of vitamin B6 in different mass fraction of aqueous UA (*w*1) at 298.15 K, 303.15 K and 308.15 K respectively**

| Solution | $(\eta_r - 1)/\sqrt{m}$ 298.15K | √m | *A* / kg$^{1/2}$·mol$^{-1/2}$ At 298.15K | *B* / kg·mol$^{-1}$ At 298.15K |
|---|---|---|---|---|
| For 1*10^(-5)m solutions | | | | |
| Pure | | 0.002125 | 0.006 | 0.007 |
| 1st | 1.26E-05 | 0.00563 | | |
| 2nd | 2.52E-05 | 0.01126 | | |
| 3rd | 3.77E-05 | 0.01689 | | |
| 4th | 5.02E-05 | 0.02252 | | |
| 5th | 7.51E-05 | 0.03378 | | |
| 6th | 9.13E-05 | 0.041155 | | |
| For 2*10^(-5)m solutions | | | | |
| Pure | | 0.0027 | 0.006 | 0.005 |
| 1st | 1.51E-05 | 0.006755 | | |
| 2nd | 3.01E-05 | 0.01351 | | |
| 3rd | 4.5E-05 | 0.02027 | | |
| 4th | 5.99E-05 | 0.027025 | | |
| 5th | 7.73E-05 | 0.03492 | | |
| 6th | 8.95E-05 | 0.040535 | | |
| For 3*10^(-5)m solutions | | | | |
| Pure | | 0.0225 | 0.003 | 0.005 |
| 1st | 1.24E-05 | 0.00563 | | |
| 2nd | 2.48E-05 | 0.01126 | | |
| 3rd | 3.71E-05 | 0.01689 | | |
| 4th | 4.94E-05 | 0.02252 | | |
| 5th | 7.39E-05 | 0.03378 | | |
| 6th | 7.9E-05 | 0.03617 | | |
| For 1*10^(-5)m solutions | | | | |
| Pure | | 0.002125 | 0.006 | 0.007 |
| 1st | 1.26802E-05 | 0.00563 | | |

| Solution | $(\eta_r - 1)/\sqrt{m}$ 298.15K | √m | $A$ / $kg^{1/2}\cdot mol^{-1/2}$ At 298.15K | $B$ / $kg\cdot mol^{-1}$ At 298.15K |
|---|---|---|---|---|
| 2nd | 2.53034E-05 | 0.01126 | | |
| 3rd | 3.787E-05 | 0.01689 | | |
| 4th | 5.03803E-05 | 0.02252 | | |
| 5th | 7.54018E-05 | 0.03378 | | |
| 6th | 9.16592E-05 | 0.041155 | | |
| For $2*10^{\wedge(-5)}$m solutions | | | | |
| Pure | | 0.0027 | 0.006 | 0.005 |
| 1st | 1.51457E-05 | 0.006755 | | |
| 2nd | 3.02237E-05 | 0.01351 | | |
| 3rd | 4.52455E-05 | 0.02027 | | |
| 4th | 6.01893E-05 | 0.027025 | | |
| 5th | 7.76E-05 | 0.03492 | | |
| 6th | 8.9878E-05 | 0.040535 | | |
| For $3*10^{\wedge(-5)}$m solutions | | | | |
| Pure | | 0.0225 | 0.003 | 0.007 |
| 1st | 1.2567E-05 | 0.00563 | | |
| 2nd | 2.5078E-05 | 0.01126 | | |
| 3rd | 3.75333E-05 | 0.01689 | | |
| 4th | 4.99335E-05 | 0.02252 | | |
| 5th | 7.47345E-05 | 0.03378 | | |
| 6th | 7.98455E-05 | 0.03617 | | |
| Solution | $(\eta_r - 1)/\sqrt{m}$ 308.15K | √m | $A$ / $kg^{1/2}\cdot mol^{-1/2}$ At 308.15K | $B$ / $kg\cdot mol^{-1}$ At 308.15K |
| For $1*10^{\wedge(-5)}$m solutions | | | | |
| Pure | | 0.002125 | 0.006 | 0.007 |
| 1st | 1.27E-05 | 0.00563 | | |
| 2nd | 2.54E-05 | 0.01126 | | |
| 3rd | 3.8E-05 | 0.01689 | | |
| 4th | 5.06E-05 | 0.02252 | | |
| 5th | 7.57E-05 | 0.03378 | | |
| 6th | 9.21E-05 | 0.041155 | | |
| For $2*10^{\wedge(-5)}$m solutions | | | | |
| Pure | | 0.0027 | 0.006 | 0.005 |
| 1st | 1.52E-05 | 0.006755 | | |
| 2nd | 3.04E-05 | 0.01351 | | |
| 3rd | 4.54E-05 | 0.02027 | | |
| 4th | 6.05E-05 | 0.027025 | | |
| 5th | 7.79E-05 | 0.03492 | | |
| 6th | 9.03E-05 | 0.040535 | | |
| For $3*10^{\wedge(-5)}$m solutions | | | | |
| Pure | | 0.0225 | 0.003 | 0.005 |
| 1st | 1.26E-05 | 0.00563 | | |
| 2nd | 2.52E-05 | 0.01126 | | |
| 3rd | 3.77E-05 | 0.01689 | | |
| 4th | 5.02E-05 | 0.02252 | | |
| 5th | 7.51E-05 | 0.03378 | | |
| 6th | 8.02E-05 | 0.03617 | | |

**Table 7.4. Conductance data of PY in UA solution (i.e., 10m (M) VITAMIN B6 SOLN+2*10^(-5) URIC ACID SOLUTIONS)**

| NO | VOL OF VITAMIN SOLN | VOL OF UA | TOTAL VOL | CONDUCTANCE |
|---|---|---|---|---|
| **1** | 10 | 0 | 10 | 134 |
| **2** | 10 | 1 | 11 | 123 |
| **3** | 10 | 2 | 12 | 117 |
| **4** | 10 | 3 | 13 | 112 |
| **5** | 10 | 4 | 14 | 109 |
| **6** | 10 | 5 | 15 | 105 |
| **7** | 10 | 6 | 16 | 102 |
| **8** | 10 | 7 | 17 | 99 |
| **9** | 10 | 8 | 18 | 96 |
| **10** | 10 | 9 | 19 | 94 |
| **11** | 10 | 10 | 20 | 91 |
| **12** | 10 | 11 | 21 | 89.2 |
| **13** | 10 | 12 | 22 | 87.2 |
| **14** | 10 | 13 | 23 | 85 |
| **15** | 10 | 14 | 24 | 83.7 |
| **16** | 10 | 15 | 25 | 81.1 |
| **17** | 10 | 16 | 26 | 79.7 |
| **18** | 10 | 17 | 27 | 78.6 |
| **19** | 10 | 18 | 28 | 76.7 |
| **20** | 10 | 19 | 29 | 75.2 |

**Table 7.5. Experimental values of refractive index ($\eta_D$), molar refraction (R) of PY in the different mass fractions of aqueous uric acid solutions at 298.15K**

| M/mol kg−1 | $\eta_D$ | $R_M$ |
|---|---|---|
| PURE URIC ACID SOLUTION 1*10⁻5(M) | 1.3486 | 0.000914 |
| 1st | 1.3466 | 0.002408 |
| 2nd | 1.3462 | 0.00481 |
| 3rd | 1.3451 | 0.007194 |
| 4th | 1.3439 | 0.00956 |
| 5th | 1.3435 | 0.014325 |
| 6th | 1.3416 | 0.017363 |
| PURE URIC ACID SOLUTION 2*10⁻5(M) | 1.3440 | 0.001147 |
| 1st | 1.3442 | 0.002871 |
| 2nd | 1.3441 | 0.00574 |
| 3rd | 1.3434 | 0.008595 |
| 4th | 1.3433 | 0.011455 |
| 5th | 1.3431 | 0.014791 |
| 6th | 1.3431 | 0.017168 |
| PURE URIC ACID SOLUTION 3*10⁻5(M) | 1.3439 | 0.009557 |
| 1st | 1.3439 | 0.002391 |
| 2nd | 1.3437 | 0.004779 |
| 3rd | 1.3435 | 0.007164 |
| 4th | 1.3434 | 0.009547 |
| 5th | 1.3429 | 0.014301 |
| 6th | 1.3413 | 0.015621 |

## Figures

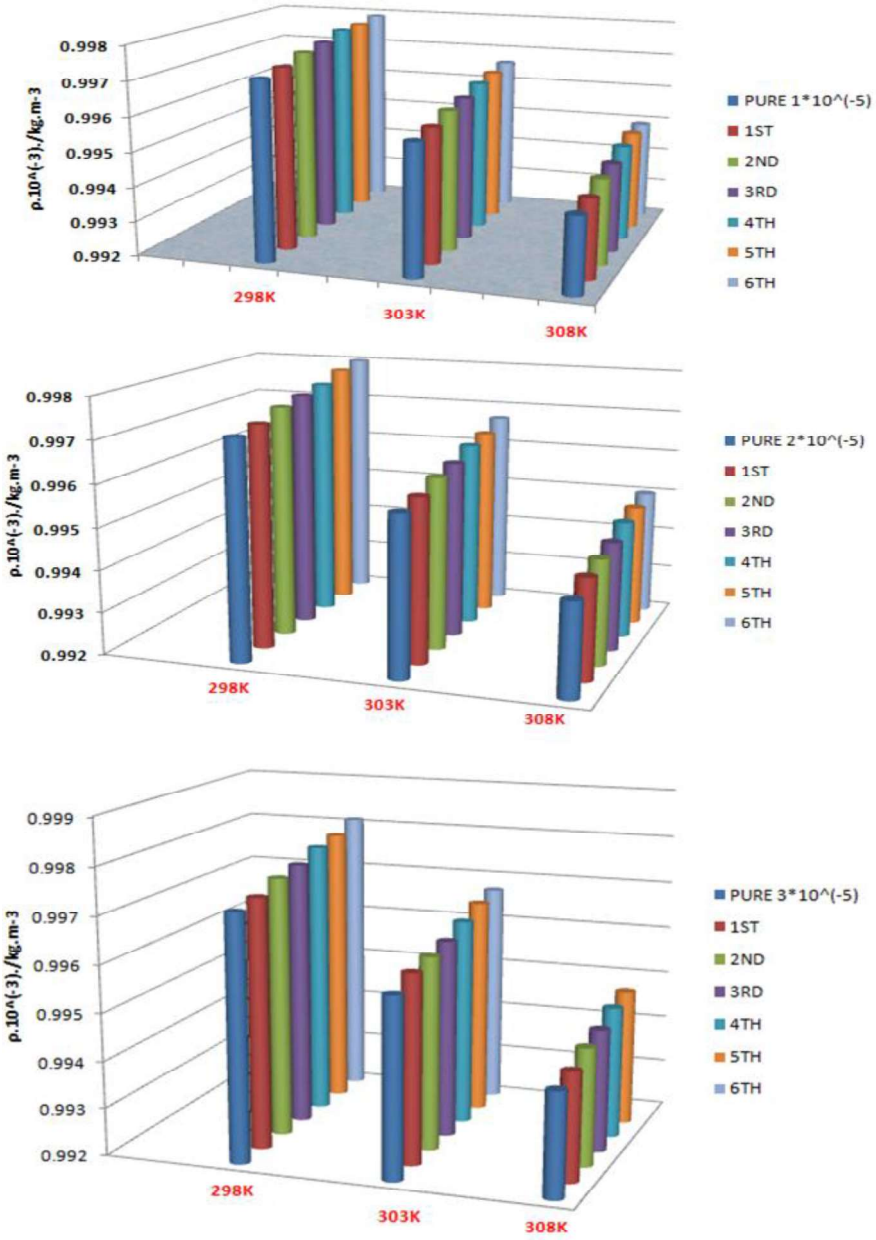


**Figure7 1. Plot of the variation of density (ρ) of solutions as a function of molality (m) for UA-$H_2O$ solutions of pyridoxine at T = 298.15 K, 303.15K, 308.15K.**

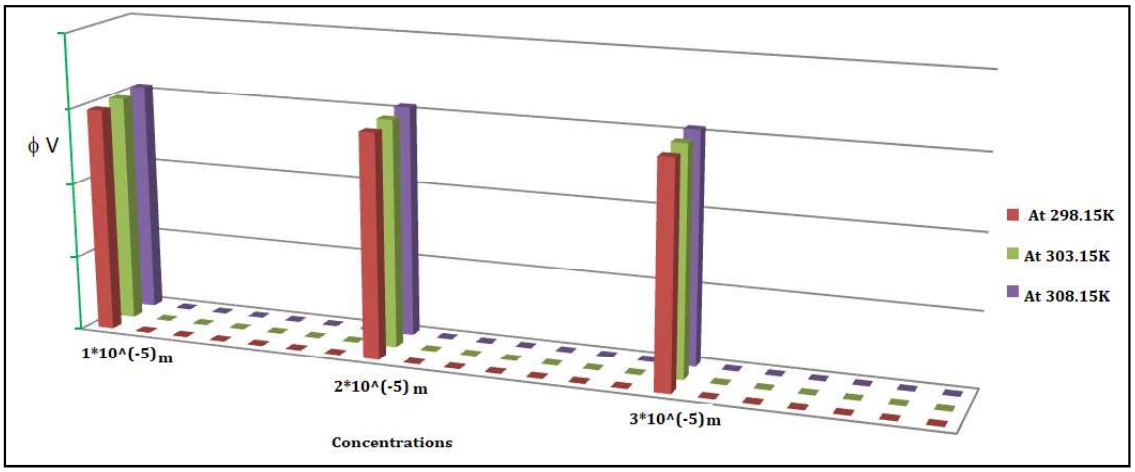


**Figure 7.2. Plot of the variation $\phi_V$ of solutions as a function of molality (m) for UA-$H_2O$ solutions of pyridoxine at T = 298.15 K, 303.15K, 308.15K.**

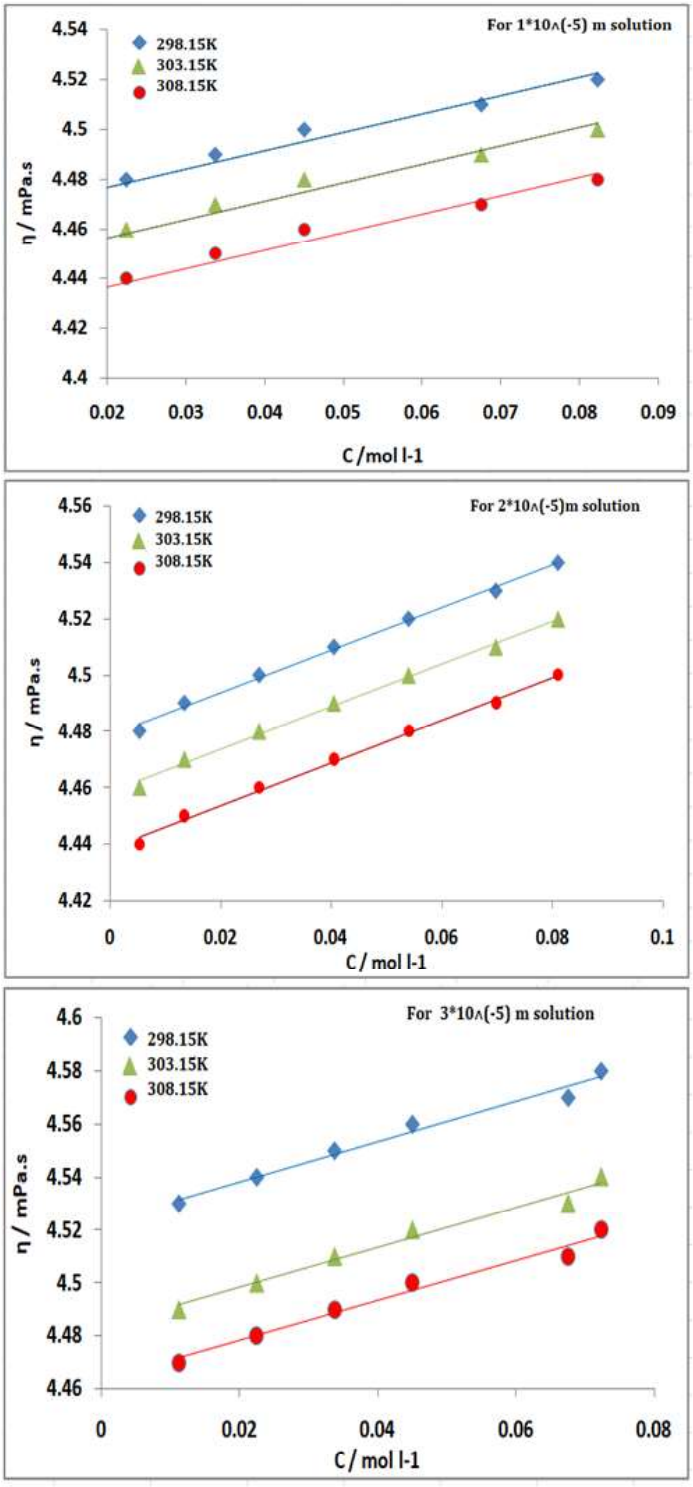


**Figure 7.3. Viscosities, η of PY in various mole fractions of UA aqueous solutions at T = 298.15 K, 303.15K, 308.15K**

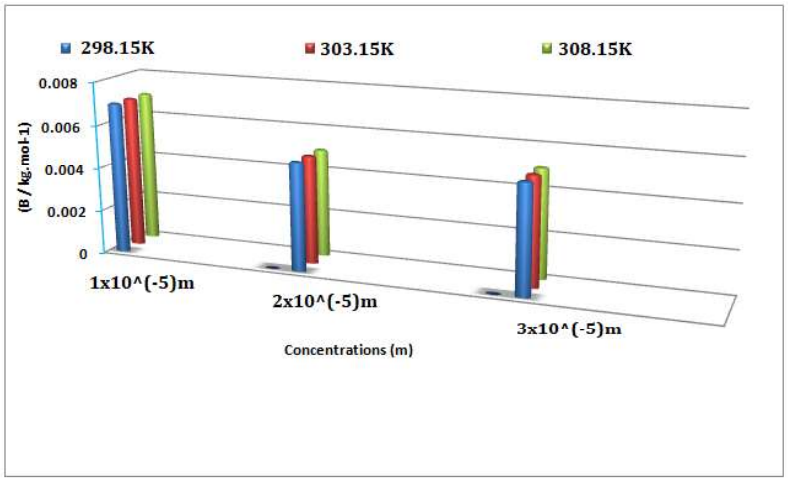


**Figure 7.4. Plots of viscosity B-coefficients for pyridoxine in different mole fractions in UA solutions at T = (298.15–308.15) K.**

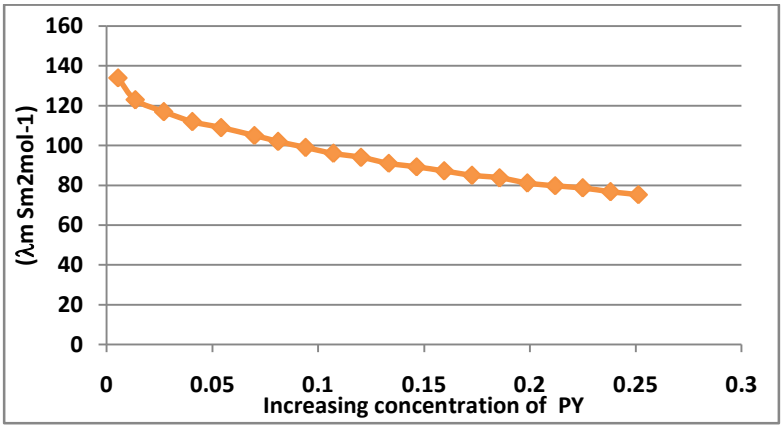


**Figure7.5: Plot of Molar conductance ( $\Lambda_m$) against concentration in aqueous PY in mass fraction of 2*10^ (-5) m of the solution**

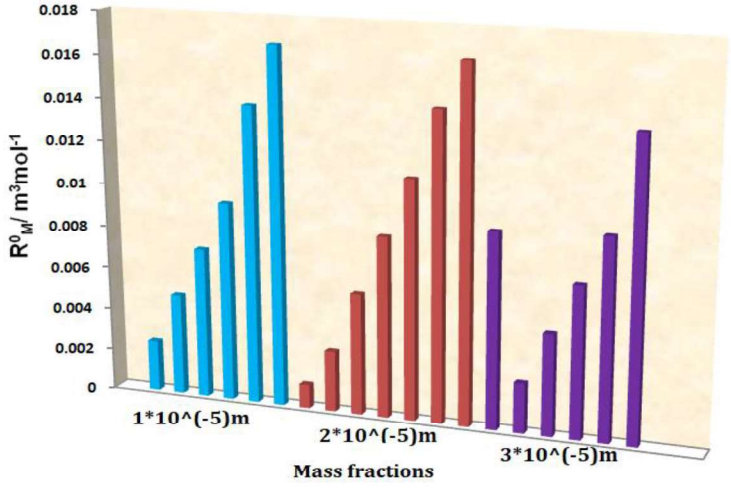


**Figure 7.6. Plot of limiting molar refraction ($R_M^0$) vs. mass fraction for 1*10^ (-5) m (sky blue), 2*10^ (-5) m (brown), 3*10^ (-5) m (purple) of PY in aqueous UA.**

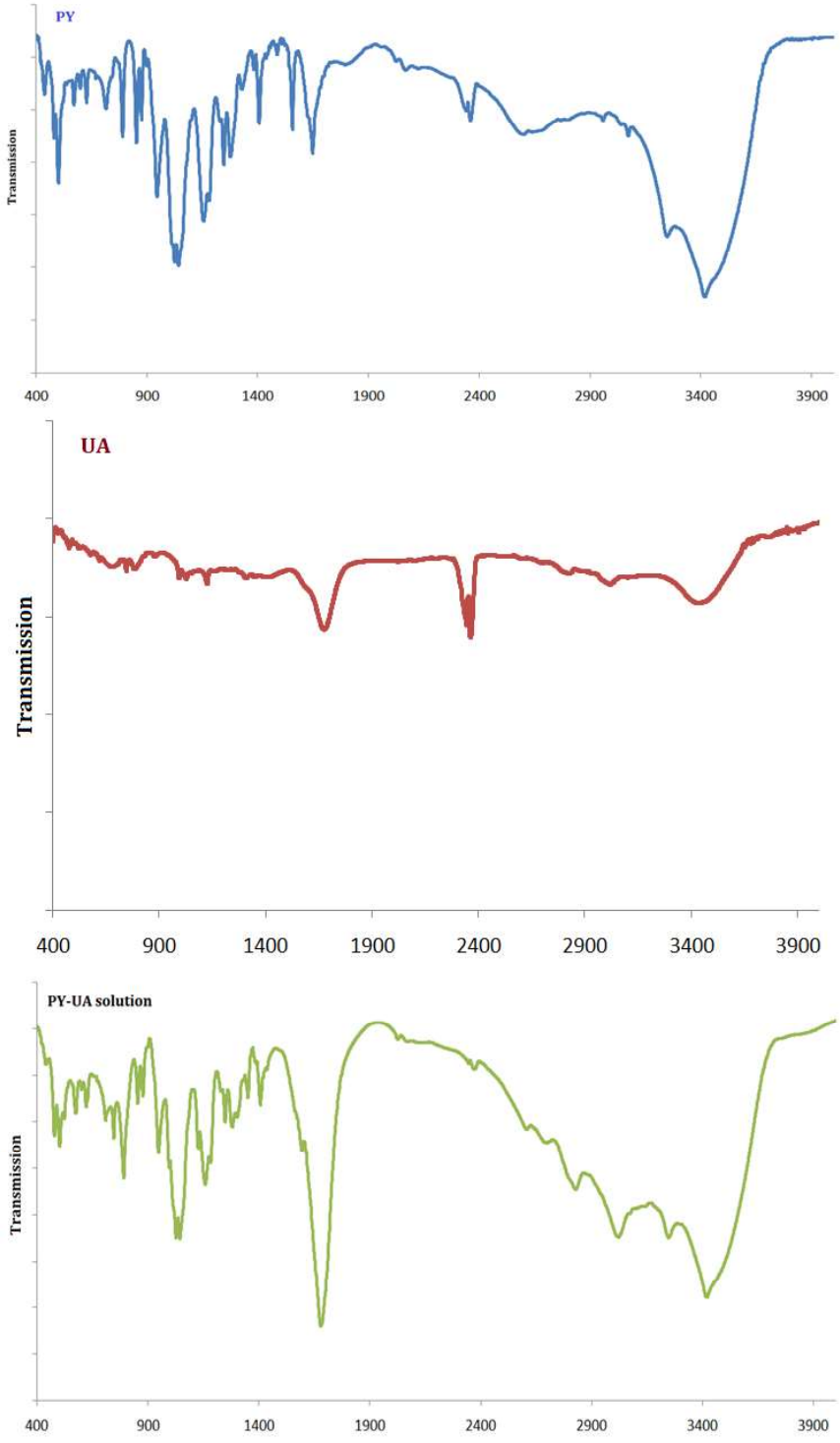


**Figure 7.7. FTIR Spectra of pure pyridoxine phosphate (PY), uric acid (UA) and mixture of PY-UA aqueous solution**

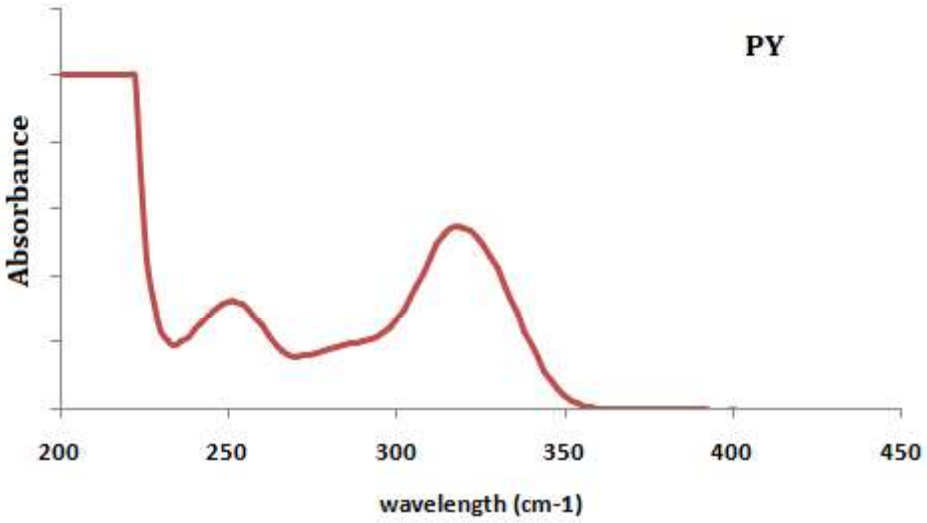


**Figure7.8. UV spectra for pure pyridoxal phosphate**

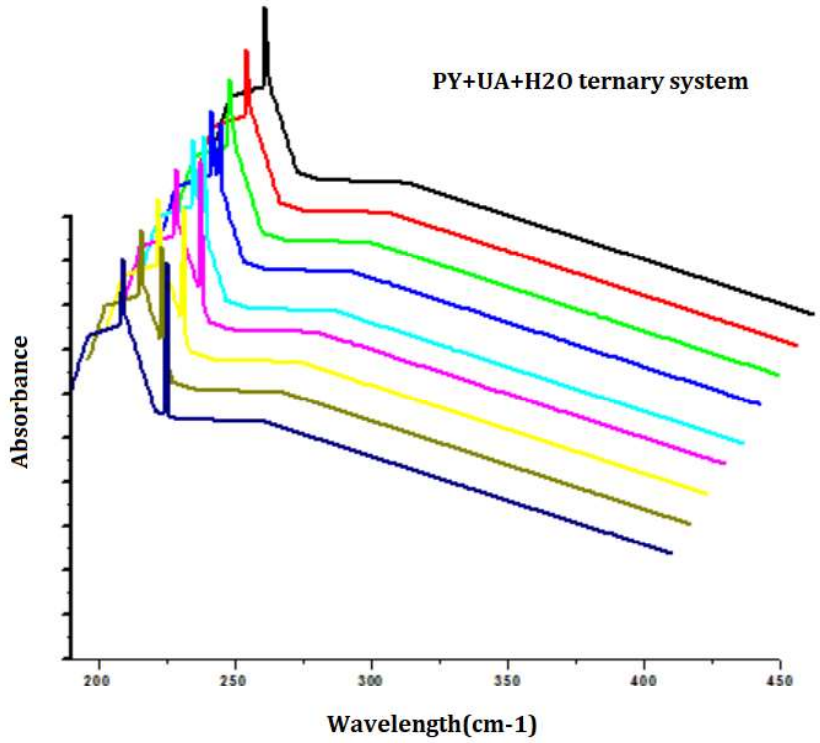


**Figure 7.9. UV spectra for pyridoxal phosphate in the presence of aqueous uric acid at room temperature**

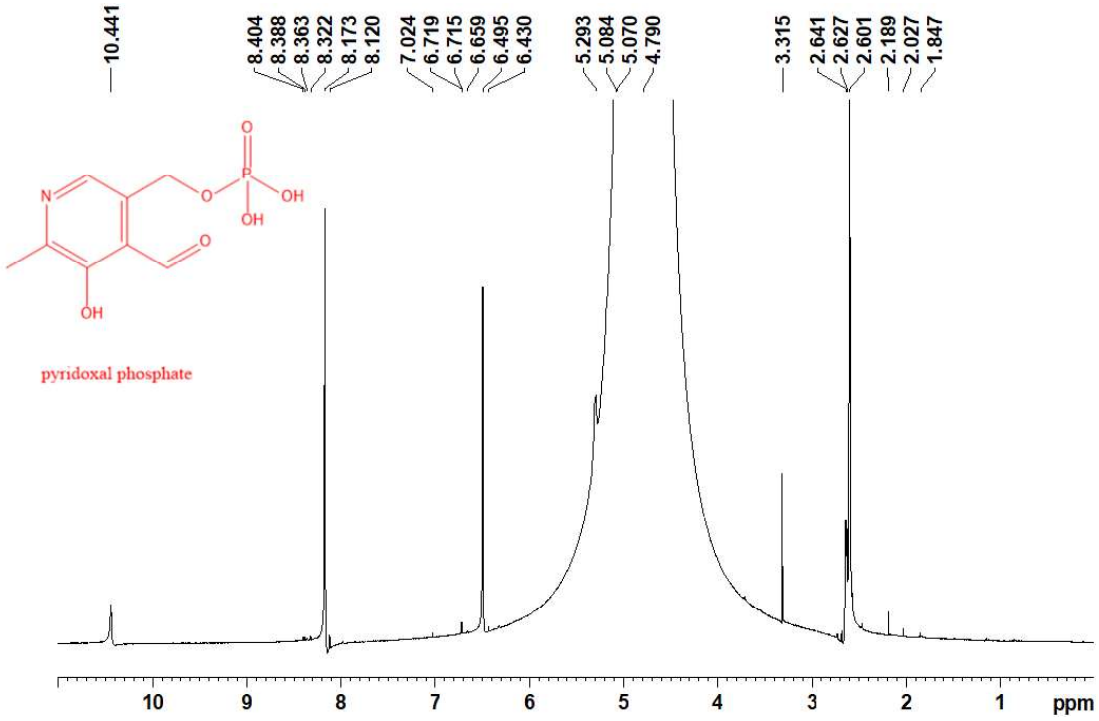


**Figure 7.10. NMR spectra for PY in $D_2O$**

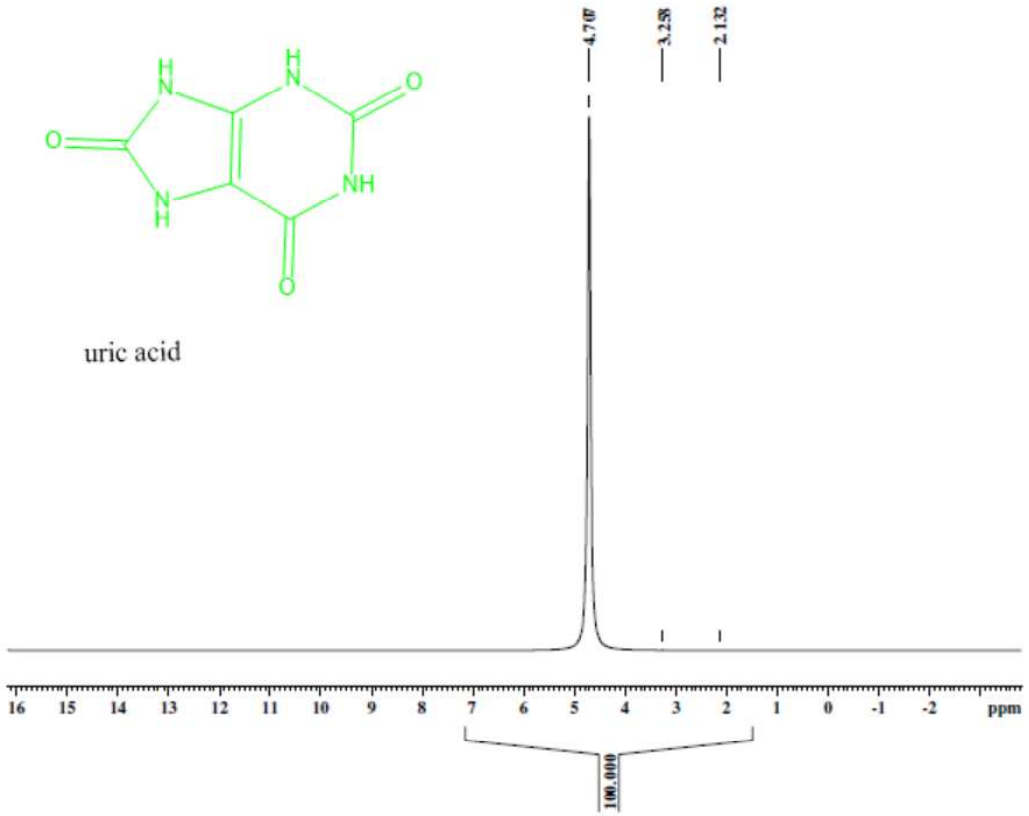


**Figure 7.11. NMR spectra for UA in $D_2O$**

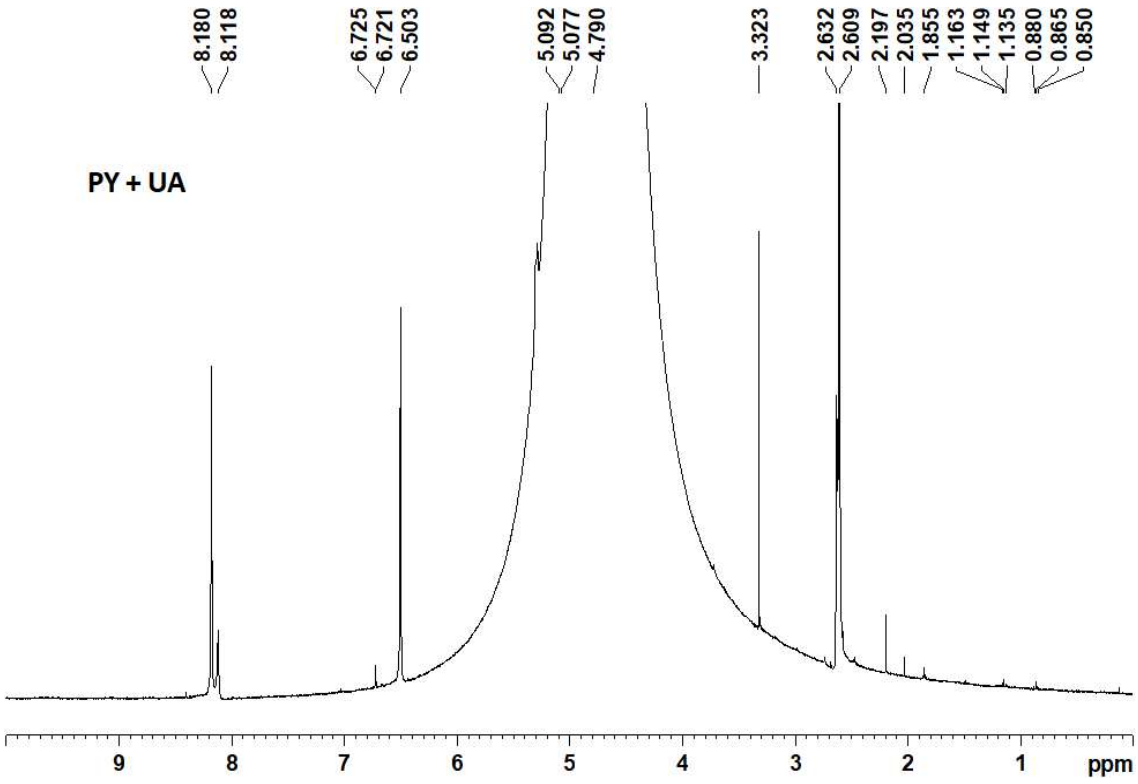


**Figure 7.12. NMR spectra for the mixture of PY + UA in $D_2O$**

**Scheme**

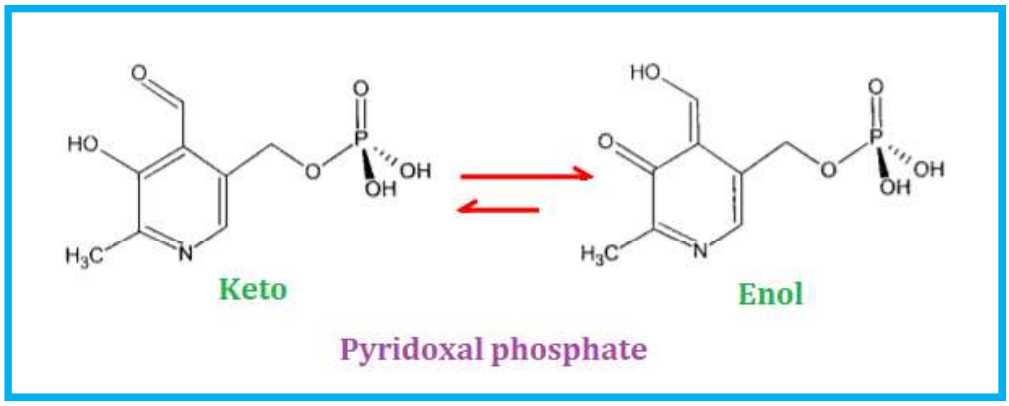


**Scheme 7.1. Representation of the exchange of hydrogen atom in PY**

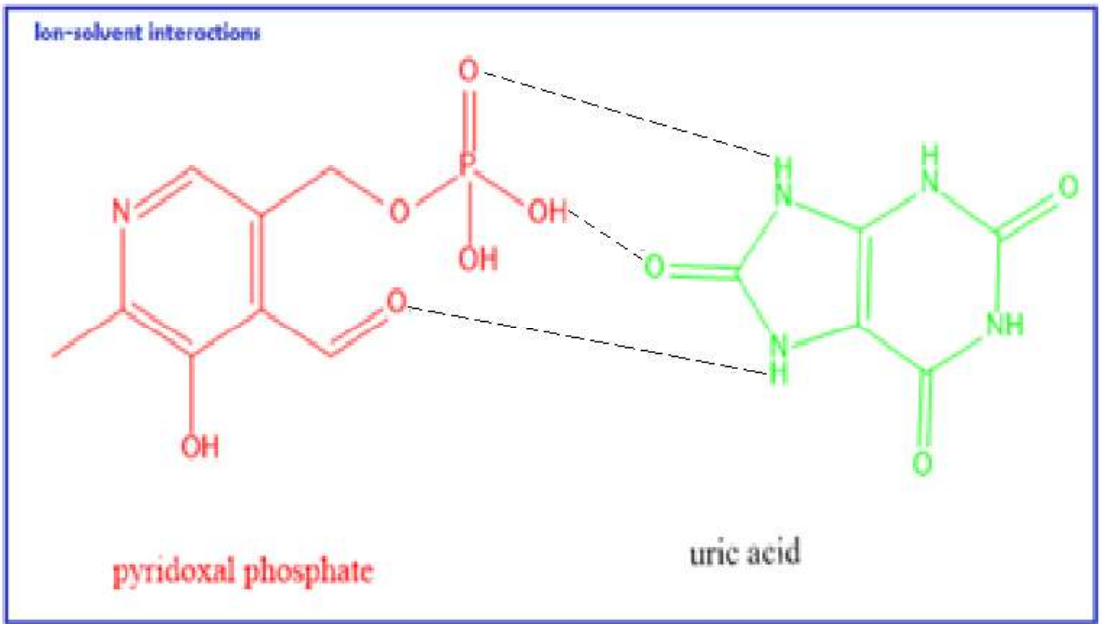


**Scheme7.2. Possible scheme for solute solvent interaction for PY-UA**

**Graphical Abstract**